Acta Neuropathol (1994) 88 : 44–54

REGULAR PAPER

X. Ye · R.I. Carp · Y. Yu · R. Kozielski · P. Kozlowski

Effect of infection with the 139H scrapie strain on the number, area and/or location of hypothalamic CRF- and VP-immunostained neurons

Received: 2 November 1993 / Revised, accepted: 7 February 1994

Abstract Scrapie is a transmissible neurodegenerative disease which shares some characteristics with Alzheimer disease (AD). Recent studies show abnormal enlargement of the adrenal glands and kidneys in 139H-affected hamsters. Using immunocytochemical techniques with antibodies to corticotropin-releasing factor (CRF) and vasopressin (VP), we observed the following: (1) a significantly higher number of CRF-immunostained neurons in the preoptic nucleus of hypothalamus of 139H-affected hamsters than controls; (2) the area of VP-immunostained (ir-VP) neurons in the lateral hypothalamus, which includes the internuclear group of magnocellular neurons and the nucleus circularis, was significantly lower for 139H-affected hamsters than for controls; and (3) no significant difference between 139H-affected and control hamsters with regard to the number of ir-VP neurons in the dorsalmedial hypothalamus (DMH), including the paraventricular hypothalamus, or the supraoptic nuclei. However, the population of ir-VP neurons in the DMH shifted to the anterior part of the hypothalamus in 139H-affected hamsters. Three-dimensional models of the immunostaining were prepared and these provide clear depictions of the changes noted. The changes in the CRF and VP systems in 139H-affected hamsters suggest that the neuroendocrine system can be affected by unconventional slow infections.

Key words Scrapie · Corticotropin-releasing factor Vasopressin · Hamster · Hypothalamus

Supported by the New York State Department of Mental Hygiene, an NIH grant AG9017, and a fellowship from the College of Staten Island/Institute for Basic Research Center for Developmental Neuroscience to X. Ye

X. Ye (✉) · R.I. Carp · Y. Yu · R. Kozielski · P. Kozlowski
New York State Institute for Basic Research
in Developmental Disabilities, 1050 Forest Hill Road,
Staten Island, NY 10314, USA

X. Ye · R.I. Carp
CSI/IBR Center for Developmental Neuroscience,
1050 Forest Hill Road, Staten Island, NY 10314, USA

X. Ye · R.I. Carp
Graduate School of the City University of New York,
33 West 42 Street, New York, NY 10036–8099, USA

Introduction

Scrapie is a neurodegenerative disease of sheep and goats [8], which begins with the animal scraping its fleece against fence posts. The disease progresses with tremors and ataxia. Death occurs within 6 weeks to 6 months without the animal demonstrating any clinical evidence of a typical viral or bacterial infection.

Recent studies have demonstrated that in some scrapie strain-mouse strain and hamster strain combinations, there is an increase in body weight that starts prior to the onset of typical motor dysfunction that signals the start of clinical disease [5]. Animals injected with scrapie strain 139H became obese during the latter part of the pre-clinical phase of disease and remained obese throughout the clinical phase. During this time, 139H-injected animals were hypoglycemic and showed lower glucose tolerance test and marked hyperinsulinemia with values of immunoreactive insulin as much as 49 times higher than those seen in controls. At autopsy, there was marked hyperplasia and hypertrophy of the cells of the islets of Langerhans [5]. The thyroid, adrenal glands, liver and kidneys were also enlarged [5]. In contrast, hamsters injected with the commonly used 263 K strain of hamster-adapted scrapie did not show any of the above changes. For example, the total body weight of these animals was the same as that of hamsters injected with normal hamster brain [17, 35].

There are a number of characteristics of scrapie and the other unconventional slow infection diseases that are shared with Alzheimer's disease (AD) and Down's syndrome. These characteristics include gliosis, neuronal loss, neurite degeneration, amyloid plaques, the

presence of host-coded aberrant fibrillar proteins (scrapie-associated fibers in unconventional slow infections, and amyloid fibers and paired helical filaments in AD) and a strong genetic influence on the pathogenesis of the disease. Furthermore, low fasting blood glucose values and hyperinsulinemia were also observed in AD patients [3]. It appears that changes in certain endocrine systems, such as the insulin system, may be an additional shared characteristic between the unconventional slow infections and AD.

Recent studies of patients with AD and normal aged individuals showed marked changes in the corticotropin-releasing factor (CRF) and/or vasopressin (VP) systems in hypothalamus [7, 12, 14]. The number of VP-immunostained (ir-VP) neurons in the paraventricular hypothalamus (PVH) was increased with aging, while AD patients did not show a similar increase. The number of ir-VP neurons in PVH in AD was 37% lower than in age-matched controls [14]. This findings suggests that the VP cells in PVH in AD fail to respond to the increase demand for VP in aging [14]. On the other hand, a dramatic increase in CRF immunostaining of perikarya and axons located in the paraventricular nucleus of the hypothalamus in AD was found [7]. In scrapie studies, we observed histopathological changes in the pituitary of 139H-affected hamsters, which included reduction in the adrenocorticotropic hormone (ACTH)-immunostained cells in the area of vacuolization of the pars distalis (Ye et al., in preparation). Together with the abnormal enlargement of the adrenal glands and kidneys in 139H-affected hamsters, these results suggested to us that the CRF/ACTH and VP systems may be affected by some scrapie agent infections.

In the current studies, we investigated the effect of scrapie infection on CRF and VP neurons in hypothalamus by free-floating-section immunostaining and used three-dimensional modeling to depict clearly the changes observed.

Materials and methods

Animals

Female, weanling, LVG/LAK hamsters were obtained from Charles River Breeding Farms (Wilmington, Mass.). Animals were maintained in a temperature- and humidity-controlled room of a reversed light:dark cycle (12:12, light on at 7:00 h) in our animal colony, and were given food and water ad libitum. Experiments were initiated in animals 1–2 weeks after their arrival.

Inocula

Two inocula were used: normal hamster brain (NHB), and scrapie strain 139H. The 139H strain was provided by Dr. Richard H. Kimberlin (Neuropathogenesis Unit, Edinburgh, UK), and is being maintained in our laboratory by hamster-to-hamster passage. The characteristics of our passaged material are exactly the same as those of the strain we originally obtained [5, 20]. Homogenization was done using 20 strokes of a hand-operated Ten-Broeck homogenizer [5]. Passages were done by routine intracerebral injection of 40 ml of a 1% brain homogenate prepared in cold (4 °C) phosphate-buffered saline (PBS). At that concentration it yielded a mean incubation period in LVG/LAK hamsters of 134 days. The clinical signs in 139H-affected hamsters include slight head bobbing and mild ataxia. All animals referred to as "control" or "normal" had been injected with a 1% homogenate of NHB.

Tissue preparation

Immunocytochemical localization of CRF and VP were performed on colchicine-treated hamsters. Colchicine enhances the CRF immunostaining in neuronal perikarya [25]. The two injection groups (NHB and 139H) consisted of ten or more animals per group. Two days prior to sacrifice animals were infused in a lateral ventricle with 15 µl colchicine solution (120 mg/15 ml) between 10:00 am and noon. Micro-injections into a lateral ventricle were carried out under general anesthesia (sodium pentobarbital 50 mg/kg, intraperitoneal injection) using a stereotactic instrument with a 30-gauge stainless steel needle (Stoelting Co.) [19]. The stereotactic coordinates used for the lateral ventricle were: A+4.3, L1.0, H+6.0. After 48 h, animals were anesthetized and perfused through the heart with a fixative containing 4% paraformaldehyde and 0.05% glutaraldehyde in 0.1 M PBS (pH 7.4). Brains were removed and placed in fixative for an additional 24 h before being transferred to 0.1 M PBS (pH 7.4). Brain coronal sections within the hypothalamus region were cut into 50-mm-thick serial sections through the forebrain from the diagonal band of Broca to the substantia nigra with a vibratome (Lancer, series 1000). The vibratome bath was filled with 0.1 M PBS at 4 °C. As each brain was cut, sections were placed sequentially in five labeled 10 ml test tubes with 0.1 M PBS at 4 °C. The sections in the first and third test tubes were treated for CRF immunostaining. The sections in the second and fourth test tubes were used for VP immunostaining. The sections in the fifth test tube were not used in this study. One section was removed from each test tube to serve as control.

Immunostaining methods

Sections for immunostaining were processed as free-floating segments using the peroxidase-antiperoxidase (PAP) method. Prior to immunostaining, sections were rinsed for at least 6 h in several changes of PBS and incubated with a solution of 10% normal sheep serum (Cappel Organon Teknika Co. Durham, N.C.) in 1% hydrogen peroxide for 30 min at room temperature to remove endogenous peroxidase. Following three rinses in PBS, the sections were then incubated in antibodies against CRF (1:500, Incstar Corporation, Stillwater, Minn.) or VP (1:2000, ICN Biomedical Inc, Ill.) for 48 h in a shaking platform at 4 °C. Sections were washed four times for 15 min each in PBS, and incubated for 2 h at room temperature in secondary antiserum of sheep anti-rabbit IgG (1:100, Cappel Organon Teknika Co.). After four washes of 15 min each in PBS, sections were incubated for 1 h in rabbit PAP (1:100, Cappel Organon Teknika Co.). Sections were washed three times 15 min each in TRIS-buffered saline (TBS, 7.45 g, pH 7.6 trizma, 8.75 g NaCl in 1 l deionized water) and washed once in TRIS buffer (TB, 7.45 g, pH 7.6 Trizma in 1 l deionized water). Peroxidase activity was revealed using 3–3'-diaminobenzidine (Sigma, 75 mg/100 ml TB with 0.01% hydrogen peroxide) for 30 min at room temperature. After washing, the sections were mounted on gelatine-coated glass slides and dehydrated, and then coverslipped with Permount (Fisher Sci).

To control for antibody specificity, three control processes were done: (1) negative control: specimens which did not contain the antigen to be stained, such as liver, were processed in the same way as the unknown; (2) reagent control: brain sections were allowed to react with a non-immune rabbit serum (1:500) instead of the primary antibody; (3) neutralized control: sections were allowed to react with an antiserum that had been exposed to an excess of the specific antigen (0.1–0.3 mg CRF or VP/ml of diluted antiserum, preincubated for 2 h at room temperature). The con-

trol tests did not show any cellular staining. The VP antiserum had been shown not to cross-react with oxytocin by the manufacturer (ICN Biomedical Inc.).

Assessment of immunostaining

Cells immunostaining in each section were counted under light microscopy using the disector principle [4]. The sampling volume was the area of the test frame multiplied by the distance between the first and last optical section. In practice, this was achieved by projecting the counting frame onto the section focusing down through the thickness of the section (50 mm). Cells for which the clearest nucleus profile or cell body falls within this volume were counted [10]. There was no attempt to discern between light-, medium- or dense-staining perikarya. Three bilateral areas containing ir-VP neurons were measured and compared: supraoptic nuclei (SON), dorsalmedial hypothalamus (DMH) and lateral hypothalamus (LHy). The SON included all perikarya above and associated with optic tracts. The DMH included all cells found along the dorsomedial aspect of the third ventricle and the perikarya located around the area of PVH. The LHy included perikarya situated in the lateral hypothalamus, dorsal to the SON, midway between DMH and SON; the LHy also included the internuclear group of magnocellular neurons [15] and the nucleus circularis [11]. The suprachiasmatic nucleus (SCN) was omitted from this study because the perikarya were small, few in number and difficult to distinguished.

The number of CRF immunostained neurons in the hypothalamus and ir-VP neurons in the SON were determined under a light microscope. The ir-VP areas in the LHy and DMH were analyzed using the Quantimet 970 image analyzer, which has a very high degree of precision and satisfies the need for increased objectivity and accuracy. Stained slides were scanned by a scanner mounted on a microscope. To maintain efficiency, the Quantimet 970 utilizes an interactive user-programmed interface, "QUIPS/MX, Version V07.00", which allows the user to establish routines for image analysis to produce the desired sensitivity and quantification.

Computer reconstructions of three-dimensional models

We also employed the Quantimet 970 image analyzer to reconstruct and analyze populations or areas of CRF and ir-VP neurons in three dimensions. The ir-VP neurons in LHy and DMH regions were easily quantitated by this method. CRF-immunostained neurons in hypothalamus and ir-VP neurons in SON were difficult to identify by the Quantimet 970 image analyzer because of high background staining, but they were easily quantitated using light microscopy.

The mapping procedure was done for all immunostained sections, which represented more than one third of the total number of sections. The immunostained neurons were reconstructed from groups of ten animals. The number of neurons on each atlas outline represented the average number of immunostained neurons in the test sections closest to the corresponding standard section. In the case of ir-VP neurons in LHy and DMH, single neurons represented a 400-μm^2 immunostained area.

For the three-dimensional models, the position of each immunostained cell was mapped on a photocopy of an atlas figure outlined from the section taken from one brain. In this study, eight outlines of sections were taken to reconstruct the brain model (see Fig. 5). The outlines of the brain were obtained from selected sections of one animal with the DL-2 microfiche projector. The atlas number of the eight standard outlines were most closely matched to the atlas figures from Sidman et al. [29].

The position of each immunostained neuron was entered into the Quantimet 970 image analyzer with its built-in digitizer, and three-dimensional reconstruction was performed using a QUIPS program. The cell bodies were plotted as small colored dots. The CRF-immunostained or ir-VP neurons for each group of animals were viewed singly or simultaneously with the other group. The ir-VP neurons in LHy, DMH and SON regions were also viewed simultaneously in control and 139H-affected groups. Photographs of displays were taken with the Nikon HP F3 model camera.

Statistical analyses

Data were analyzed using the Lotus 123 program and the CSS statistics software package. We have obtained information on the total size of the area of interest, the size of the area that shows positive staining and the optical density of the stained areas. This information was stored, statistically analyzed and compared by Student's *t*-test (unpaired *t*-test, two tailed) or analysis of variance with the data from sections obtained from animals injected with normal hamster brain. The number or areas immunostaining for CRF or VP between 139H-affected hamsters and control group was analyzed and compared at each corresponded atlas number. If *P* values were below 0.05, the Mann-Whitney U (MW-U) test (two-tailed, 0.05 level of significance) was also used to calculated differences between two groups.

Results

In normal animals, CRF-immunostained neurons have been found in different areas of brain, such as the cortex, the bed nuclei of the stria terminalis and the central nuclei of the amygdala (for review see [27]). In our studies of normal hamsters, CRF-immunostained neurons were in the basal forebrain dispersed over an area which extends in the rostra-caudal dimension from the horizontal and ventrical limbs of the diagonal band of Broca to the anterior hypothalamic area of the medial basal hypothalamus. In addition to this rostral-caudal dimension, CRF-immunostained neurons were found in specific locations with the largest accumulation in coronal sections through the cortex at layer II, the nucleus of amygdala, the diagonal band of Broca, the preoptic area and the PVH. Within the preoptic area, CRF perikarya were not confined to particular nuclear groups, but rather were heavily concentrated in the ventral preoptic zone, just dorsal of the optic chiasm, and ventral to the anterior commissure. This area is located near the preoptic periventricular nucleus, the medial preoptic nucleus, and the anterior hypothalamic area. This heavy concentration of CRF-immunostained neurons in preoptic areas is apparent in three-dimensional computer reconstructions of the population of CRF-immunostained neurons which will be documented later.

The results obtained from immunostaining of the hypothalamus of scrapie and control animals with anti-CRF and anti-VP are shown in Fig. 1–6. There are more CRF-immunostained neurons in the preoptic nucleus in 139H-affected hamsters than in control hamsters (Fig. 1). The total number of CRF-immunostained neurons in 139H-affected hamsters (19.4±3.3 neurons/section) is significantly more than that observed in control animals (7.5±1.9 neurons/section, MW-*U* test, $P<0.001$) (Fig. 3a). Figure 4a shows CRF-stained cells in relation to atlas number. At present there is no suitable atlas of hamster brain; however, since the major structures of mouse brain and hamster brain are similar, we used the

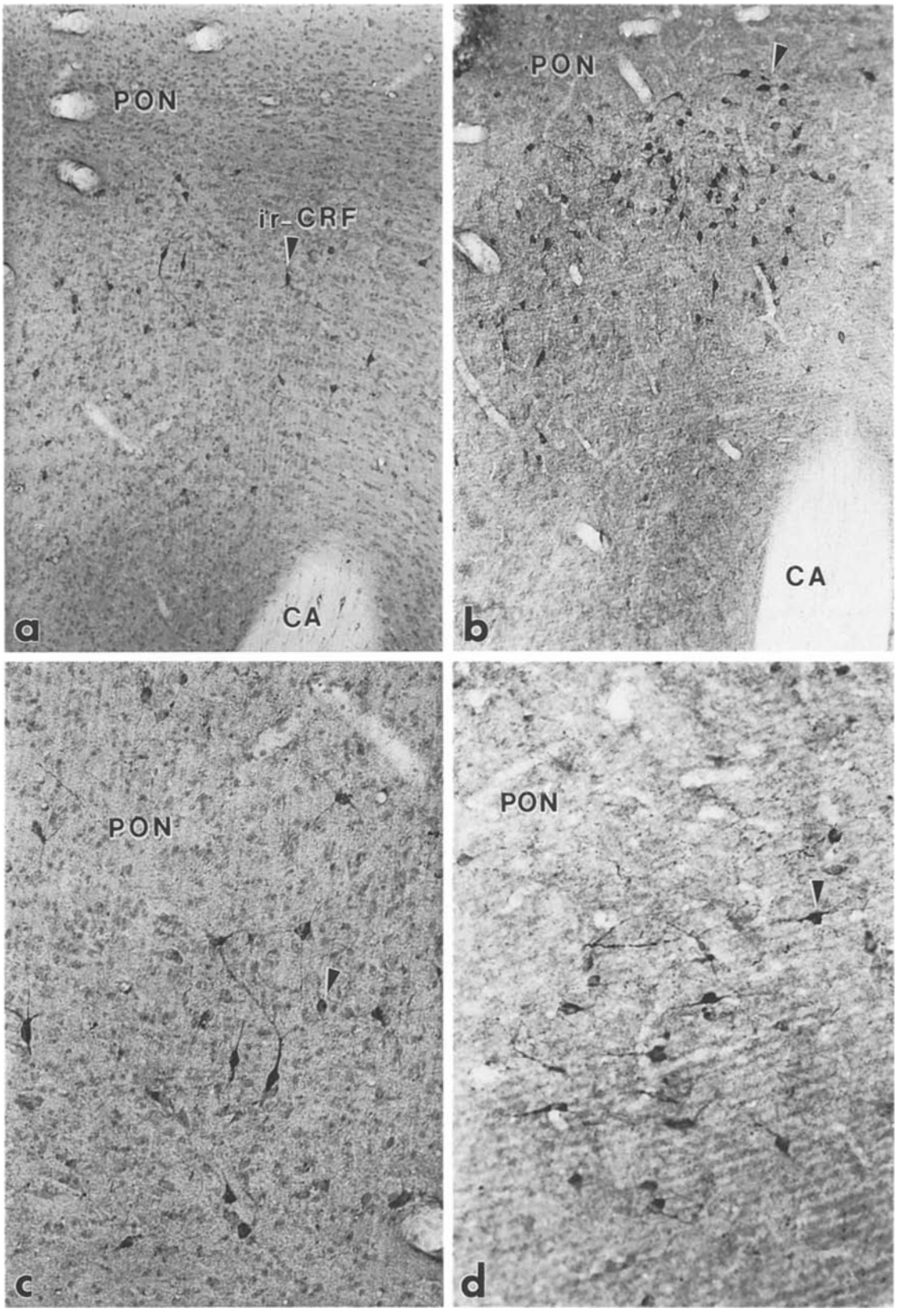

Fig. 1a–d CRF-immunostained (*ir-CRF*) cells in PON region. **a** Control hamster. **b** 139H-affected hamster. **c** Control hamster. **d** 139H-affected hamster. *Arrowhead* shows ir-CRF cells. **a**, **b**×82, **c**, **d**×164 (*CRF* corticotropin-releasing factor, *PON* preoptic nucleus, *CA* Commissura anterior, pars anterior)

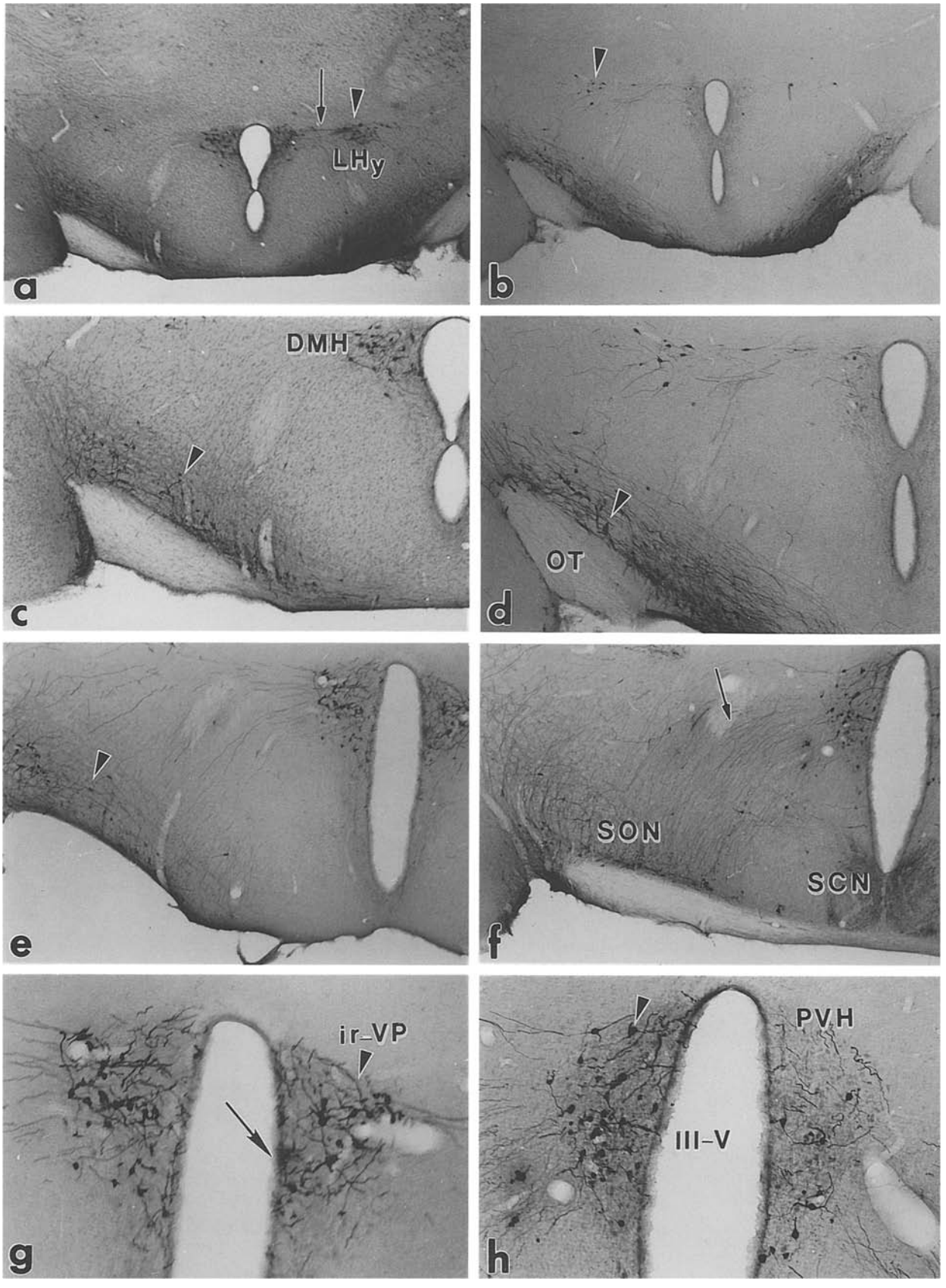
a
LHy
b
c
DMH
d
OT
e
f
SON
SCN
g
ir-VP
h
PVH
III-V

◀ **Fig. 2a–h** Vasopressin VP-immunostained (*ir-VP*) cells in the LHy, DMH, and SON regions. **a**, **c**, **e**, **g** ir-VP cells in the hypothalamus of a control hamster. **b**, **d**, **f**, **h** ir-VP cells in the hypothalamus of a 139H-affected hamster. *Arrowhead* shows ir-VP cells; *small arrow* shows ir-VP fibers projections; *medium arrow* shows that ir-VP fibers project to the wall of the third ventricle. **a**, **b**×20.5, **c–f**×41, **g**, **h**×82 (*III-V* third ventricle, *DMH* dorsomedial hypothalamus, *LHy* lateral hypothalamus, *OT* optic tract, *PVH* paraventricular hypothalamus, *SON* nucleus of supraopticus, *SCN* nucleus of suprachiasmaticus)

atlas of a mouse brain as reference [29]. We can see that the curve of CRF-stained cells in 139H-affected hamsters is higher than that in control animals. There is a peak at atlas number 30 which indicates that the number of CRF-immunostained neurons in the preoptic area of 139H-affected hamsters had increased compared to the number in control animals. This difference is evident in comparisons of computer-reconstructions of CRF neuron populations (Fig. 6a).

The ir-VP neurons are larger than those stained for CRF. Unlike CRF-immunostained neurons, which are widely distributed throughout the brain, VP-containing neurons are mainly located in three areas in the hypothalamus, namely the LHy, DMH, and SON. There are many ir-VP fiber connections between each nucleus. The immunostaining of VP containing cells in the LHy, DMH and SON is shown in Fig. 2. There was a significant decrease in the area of ir-VP in the lateral hypothalamus (LHy) of 139H-affected hamsters (2543±481 μm^2/section) compared with the area in control animals (5273±1212 μm^2/section, unpaired *t*-test, $P<0.05$) (Fig. 3b). Figure 4b shows the ir-VP area in the LHy in relation to atlas number. The curve of the ir-VP area of 139H-affected hamsters is lower than that of control animals; there is a peak at atlas numbers 34–36 in control animals, but not in 139H-affected hamsters.

The area of ir-VP in DMH of 139H-affected hamsters (7669±1800 μm^2/section) was not significantly different from the area in control animals (7997±1949 μm^2/section) (Fig. 3c). The curve of the ir-VP area in DMH as a function of atlas number of 139H-affected hamsters is almost the same as that of control animals (Fig. 4c). There is a shift of the peaks to the left in the 139H-affected hamsters, but the pattern of the curve is almost the same in the two groups.

Figure 5 demonstrates the outlines of the position of ir-VP neuronal cell bodies in the SON region. The number and distribution of ir-VP cells in control hamsters (14.7±0.2/section, Fig. 5) were not significantly different from the number and distribution in 139H-affected animals (14.4±0.3/section, distribution data not shown).

The eight outlines of the brain used in Fig. 5 were also used for the three-dimensional reconstruction models. The three dimensional reconstruction of CRF-immunostained neurons in the hypothalamus and ir-VP neurons in the LHy, DMH and SON, respectively, are

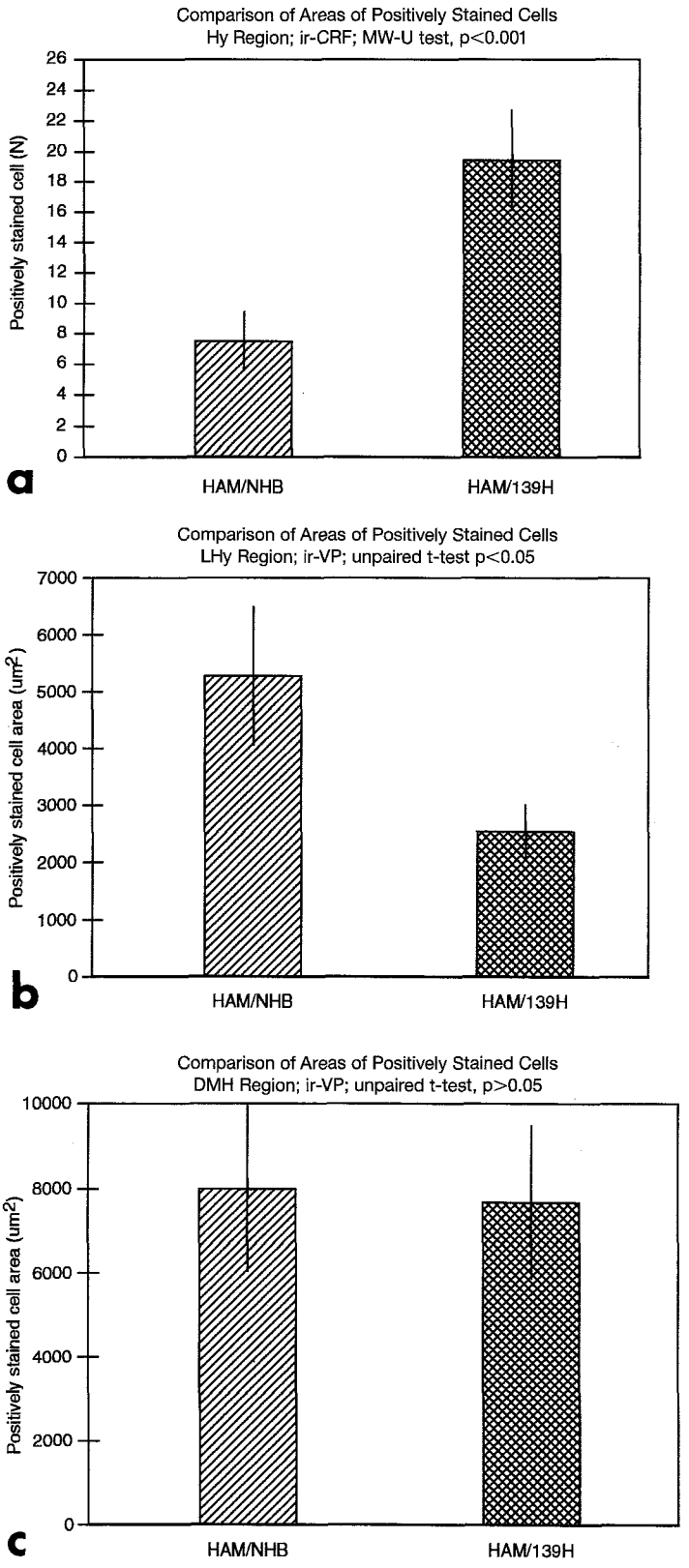

Fig. 3a–c Comparison of numbers of CRF-stained cells per section in hypothalamus (*Hy*) region and areas of ir-VP cells per section in LHy and DMH regions. **a** The number of the CRF-immunostained neurons per section in Hy area; MW-U test, $P<0.001$. **b** The area of the ir-VP neurons per section in LHy region; unpaired *t*-test, $P<0.05$. **c** The area of the ir-VP neurons per section in the DMH region; unpaired *t*-test, $P>0.05$

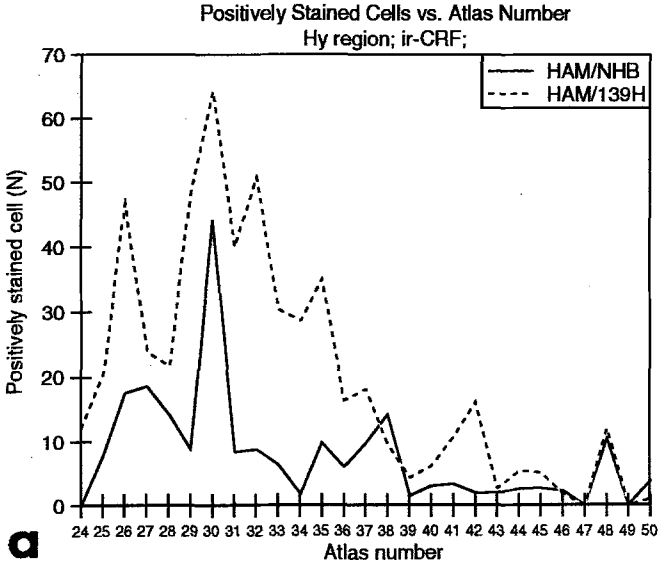

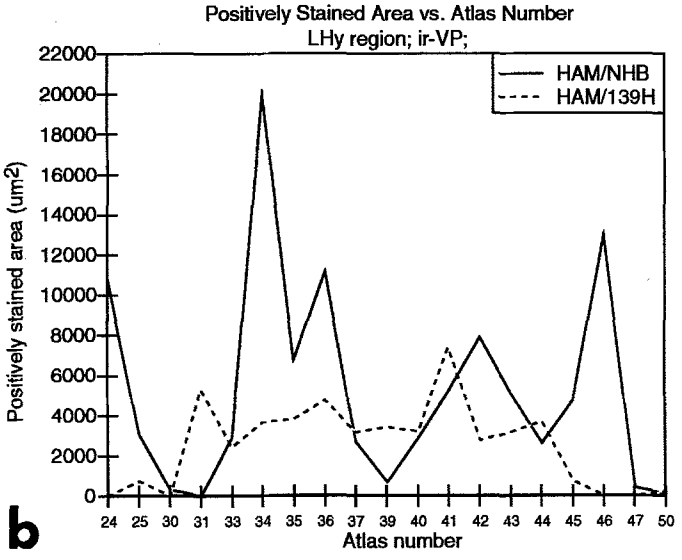

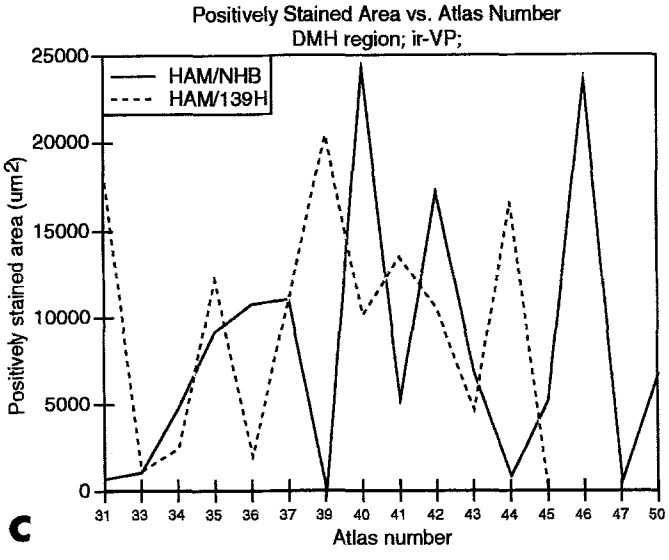

shown in Fig. 6. As noted, the population of CRF-immunostained neurons was larger in 139H-affected hamsters than in controls (Fig. 6a). As shown in Fig. 6b and c, the population of ir-VP neurons in LHy was less in 139H-affected hamsters compared to the population of neurons in control animals. The total number of ir-VP neurons in the DMH region was not significantly different from controls, but there was a shift in positively stained cells from caudal to rostral regions in scrapie positive animals. There was no significant difference in the number of ir-VP neurons in the SON region in 139H-affected hamsters compared to the number in control hamsters.

Discussion

Hamsters infected with the 139H strain of scrapie showed a significant increase in body weight compared to controls [6] and histopathological changes in the islets of Langerhans [5, 35, 36]. In addition, the thyroid, adrenal glands, liver and kidneys were enlarged [5], and there were extensive pathological changes in the pituitary of 139H-affected hamsters (Ye et al., in preparation). These studies suggest that the 139H scrapie strain induces a severe generalized endocrinopathy in hamsters.

In the present studies, there was a significant increase in the number of CRF-immunostained neurons in the preoptic area of hypothalamus in 139H-affected hamsters compared with the number in control animals. CRF secretion undergoes diurnal cycles that contribute to the maintenance of glucocorticoid rhythms. Under normal conditions, the plasma glucocorticoid levels peak around the time of awakening. They are highest in the morning for daylight-active species, and highest at the onset of darkness in nocturnal ones. In our studies, all hamsters were killed between 10:00 am and noon.

The mechanism underlying the increase in the number of CRF-immunostained neurons in the hypothalamus is not clear. One possible explanation is a complementary effect related to a reduction in ir-ACTH cells in the area of vacuolization of the pituitary in 139H-affected hamsters (Ye et al., in preparation), and the abnormal enlargement of the adrenal glands which will be discussed later. Another potential explanation is damage in the hippocampus of scrapie-positive animals. In a recent study, male Sprague-Dawley rats received stereotaxic injections of ibotenic acid or saline into the

Fig. 4a–c CRF-immunostained cells and ir-VP areas as a function of atlas number. **a** The number of CRF positive cells in Hy region in control ($n=10$) and 139H-affected hamsters ($n=10$) is plotted as a function of atlas number. **b** The curve of ir-VP area in the LHy region of 139H-affected hamsters ($n=10$) is compared with that in control animals ($n=10$). **c** The curve of ir-VP area in DMH region of 139H-affected hamsters ($n=10$) is compared with that in control animals ($n=10$)

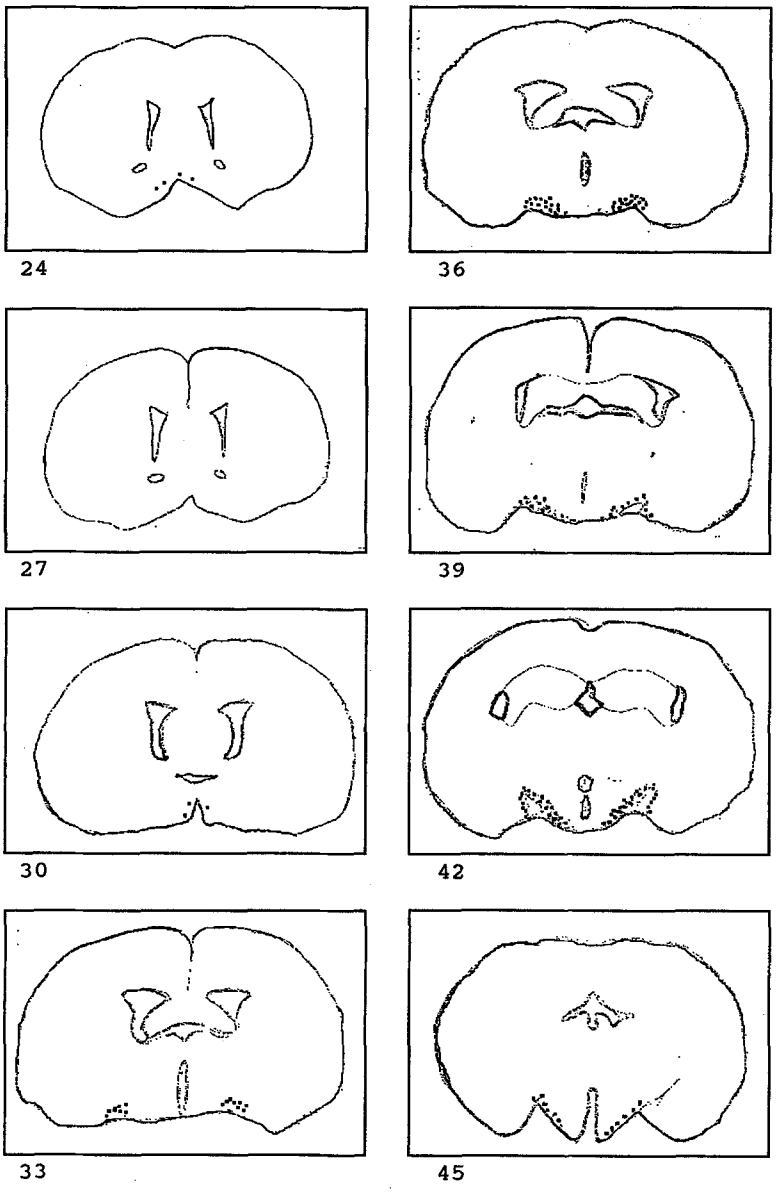

Fig. 5 Outlines of the position of ir-VP neurons in supraoptic nuclei (SON) region. ir-VP neurons were mapped onto outlines of the atlas figures according to Sidman et al. [29]. The dots represent ir-VP neurons in the SON region. The outlines of the atlas figures were scanned into a NEC Powermate/SX computer, using Hewlett Packard ScanJet. The graphics were first obtained using SCAN GALLERY 5.0 and then edited using Microsoft Windows Paintbrush. There was no significant different between control and 139H-affected hamsters

ventral subiculum or ventral hippocampus [16]. Animals with damage confined to the ventral hippocampus (including portions of CA1, CA3 and the dentate gyrus) had increased levels (30–80%) of CRF mRNA in the medial parvocellular paraventricular nucleus compared to controls [16]. These studies suggest the existence of distinct hippocampal pathways involved in tonic regulation of the hypothalamus-pituitary-adrenal (HPA) axis and in modulation of the magnitude of the stress response [16]. In other scrapie strain-host combinations a decrease in hippocampal neurons has been described [28], but this parameter has not been assessed in 139H-affected hamsters.

In AD, different patterns of changes can be seen in the CRF system, several reports have shown that CRF levels are decreased in regions other than the hypothalamus. Using radioimmunoassay techniques, Whitehouse et al. [33] showed that CRF levels were lower in AD than in age-matched controls in frontal, temporal and occipital regions of the neocortex. In another study, CRF immunostaining was reduced in the amygdala and cortex of AD patients, while in these same patients there was an up-regulation of CRF receptors in the cerebral cortex [33]. In contrast, it has been found that there is a dramatic increase in CRF immunostaining of

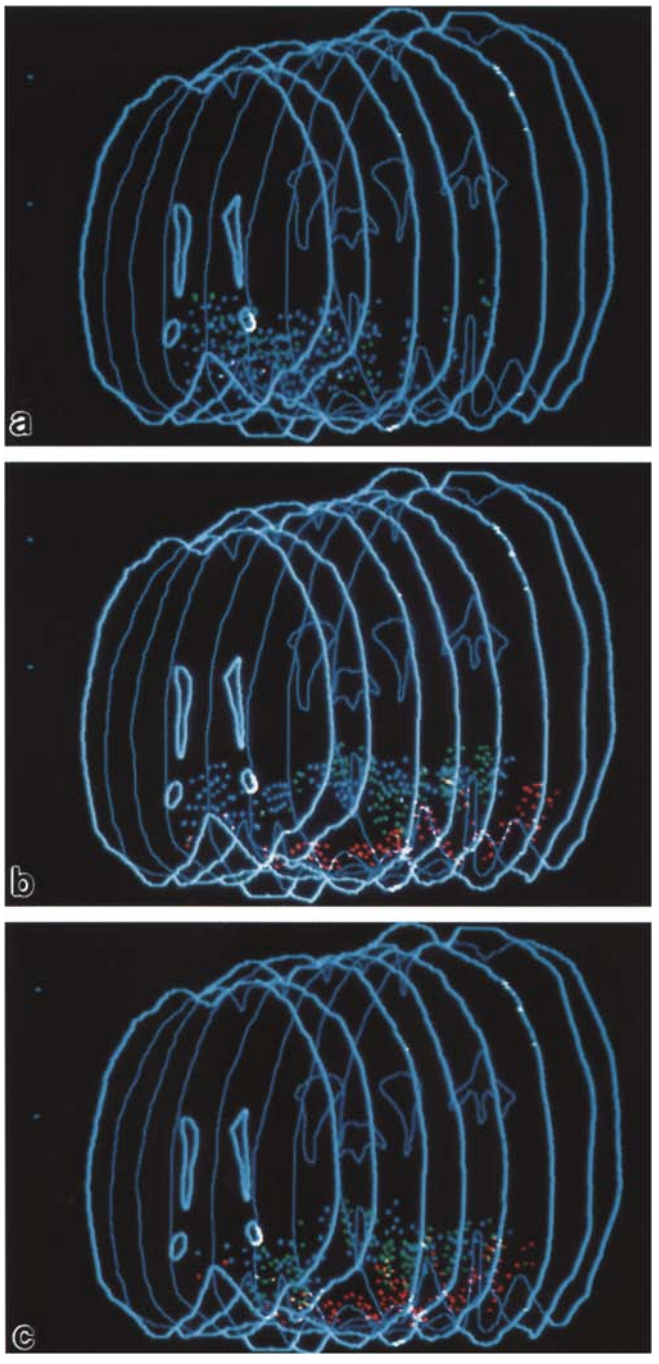

Fig. 6a–c Comparison of CRF-immunostained and ir-VP neurons in control and 139H-affected hamsters with three-dimensional reconstruction models. Three-dimensional views of CRF-immunostained and ir-VP neurons in the brains of control and 139H-affected hamsters. The models of the brain are viewed from a 60° rotation around the y axis; rostral (*left*); caudal (*right*). The cortices are transparent so that interior structures and immunostained neurons can be viewed. The right edge of the cortex is *white*; the left edge of the cortex is *blue*. Parts of the ventricles and of the commissura anterior, pars anterior are also colored *blue* or *white* to provide a frame of reference. The average population of immunostained neurons in both control (n=10) and 139H-affected hamster groups (n=10) is expressed simultaneously in the same model. **a** CRF-immunostained neurons in Hy; *green*: control, *blue*: 139H-affected. **b** ir-VP neurons in control animals. LHy: *blue*; DMH: *green*; SON: *red*. **c** ir-VP neurons in 139H-affected animals. LHy: *blue*; DMH: *green*; SON: *red*

perikarya and axons located in the paraventricular nucleus of the hypothalamus [7]. In another experiment, CRF levels in cerebrospinal fluid of AD patients were significantly higher than in controls [22]. The above studies suggest an over-activity of the HPA axis in AD [7, 22].

The similarity in the change in the CRF system in the hypothalamus of humans with AD and scrapie-affected hamsters is an addition to a number of similarities between these two diseases: astrocytosis, microgliosis, neuronal and neurite degeneration and amyloid plaques. In addition, there is a pronounced damage of neurons in the hippocampus in both AD [21, 31] and scrapie [28]. If the hypothesis that the ventral hippocampal structures play a role in modulation of HPA function [16, 32] is correct, it may explain the mechanism involved in the significantly increased number of CRF immunostained neurons in the hypothalamus of both AD humans and 139H-affected hamsters.

There was a significant decrease in the area of ir-VP neurons in the lateral hypothalamus (LHy) of 139H-affected hamsters compared with control animals, but there were no significant differences observed in the DMH and SON. The different change patterns in the VP system were also seen in aging humans and in AD patients. In senescence and in AD brain a marked decrease in total cell numbers and in the number of ir-VP neurons was observed in the SCN; these neurons may regulate circadian rhythmicity [30]. In contrast, total cell numbers in the SON and PVH, which project to the posterior lobe (pars nervosa) of the pituitary, are even activated in aging, and the PVH remains stable in AD [12, 14]. Since the renal sensitivity to VP decreases during aging, the authors suggest that the increase in VP production in the SON and PVH in senescence might be due to kidney changes [14].

The extensive changes observed in liver, kidney and endocrine organs, e.g., adrenal glands, raise the issue of the primary event that leads to these changes. An important question is whether that event occurs centrally, i.e., in the brain, or locally in these organs. At this time, we can not answer this question. Thus far, the data obtained for infectivity and for the scrapie disease-specific protease resistant protein (PrP^{Sc}) indicate a comparatively low level (in comparison with the brain) of scrapie replication in these peripheral organs. For example, compared to brain, the infectivity level in pancreas is 6000- to 10 000-fold lower [6]. Adrenal glands in mice infected with the ME7 and 139A scrapie strains had much lower titers than brains, the titers representing 0.06 and 1%, respectively, of the titer in brain [18]. The titer for kidney in 263K-infected hamsters was approximately one million-fold less than brain (Carp and Robakis, unpublished). The levels of PrP in the pancreas, adrenal gland and kidney are much lower [1, 35]. Finally, liver and kidney have extremely low infectivity [9] and there does not appear to be any PrP in livers from control animals [1, 24]. It is most likely that the pathological changes found in the pancreatic islets, adrenal

glands, liver and kidneys in 139H-affected hamsters are the result of specific targeting effects in CNS by scrapie [5, 35, 36] and that the changes in the peripheral organs are a function of brain neuronal death and dysfunction.

The hypothalamo-pituitary system is important in regulating adrenal gland endocrine function and kidney antidiuretic and natriuresis functions. CRF and VP are released from the hypothalamic nerve fiber endings around the capillaries of the external zone of median eminence and reach the anterior lobe (pars distalis) of the pituitary through the special portal capillary plexus. They both can stimulate the release of ACTH, which can increase the synthesis and release of steroids from the adrenal cortex [34]. VP released from the hypothalamo-neurohypophyseal system is an important hormone in regulating the kidney diuresis function. VP also plays an important role in regulation of blood pressure, plasma osmolality and blood coagulation [14]. The abnormal CRF/ACTH and VP activity would certainly affect adrenal gland and kidney functions as well as be the cause of the changes seen in parenchymal cells and in organ structures in 139H-affected hamsters. The changes in CRF and VP immunostaining may not be a direct effect of scrapie infection, but rather may be the result of secondary effects due to pathological changes in other neurons or other cells. It has been found that many neurotransmitters, hormones, growth factors as well as nutrients such as glucose can affect CRF and/or VP systems [34], and these factors could act on the CRF and VP neurons from another location in which the scrapie agent is having its primary effect.

It has been shown that canine distemper virus (CDV) causes obesity in a proportion of mice that survive beyond the first few weeks following infection [23]. The syndrome of CDV-affected mice is very similar to that of 139H-affected hamsters including pronounced hyperplasia and moderate hypertrophy of fat cells; reduced brain, uterus, ovary and prostrate weights; and increased liver, kidney and pancreas weights, with greatly enlarged pancreatic islet tissue. These obese animals were also hyperinsulinemic. Examination of the brains of these mice revealed a significant reduction in tyrosine hydroxylase immunoreactivity and in pro-opiomelanocortin mRNA-positive perikarya in the arcuate area. Nagashima et al. [23] suggested that the loss of critical populations of hypothalamic neurons as a result of CDV infection led ultimately to the development of morbid obesity.

Scrapie can induce obesity in sheep [26], mice [4] and hamsters [5]. The relationship between brain lesions and obesity is not clear. It has been known for many years that a lesion in the ventromedial hypothalamus can cause obesity in rats; however, the mechanism of this hypothalamic obesity is still not clear. Scrapie-induced obesity may share the same anatomical focus. Because scrapie-like agents are also found in humans, it is possible that a subset of morbidly obese humans, who are also diabetic and/or hyperinsulinemic, are infected by some kind of slow infection agent.

Acknowledgements We thank Ms. Jennifer DeKolf for editing and excellent assistance in preparation of this manuscript. We wish to thank Ms. Sharon Callahan and Mr. Richard Weed for their collaboration in this study. We appreciate the assistance of Ms. Mary Ellen Cafaro with the layout of figures. We also wish to thank Ms. Maureen Marlow for critical reading of this manuscript.

References

1. Bendheim PE, Brown HR, Rudelli RD, Scala LJ, Goller NL, Wen GY, Kascsak RJ, Cashman NR, Bolton DC (1992) Nearly ubiquitous tissue distribution of the scrapie agent precursor protein. Neurology 42: 149–156
2. Braendgaard H, Evans SM, Howard CV, Gundersen HJG (1989) The total number of neurons in the human neocortex unbiasedly estimated using optical disectors. J Microsc 157: 285–304
3. Bucht G, Adolfsson R, Lithner F, Winblad B (1983) Changes in blood glucose and insulin secretion in patients with senile dementia of Alzheimer type. Acta Med Scand 213: 387–392
4. Carp RI, Callahan SM, Sersen EA, Moretz RC (1984) Preclinical changes in weight of scrapie-infected mice as a function of scrapie agent-mouse strain combination. Intervirology 21: 61–69
5. Carp RI, Kim YS, Callahan SM (1990) Pancreatic lesions and hypoglycemia-hyperinsulinemia in scrapie-injected hamsters. J Infect Dis 161: 462–466
6. Carp RI, Ye X, Kascsak RJ, Rubenstein R (1994) The nature of the scrapie agent: biological characteristics of scrapie in different scrapie strain-host combinations. Ann NY Acad Sci (in press)
7. De Souza EB (1988) CRH defects in Alzheimer's and other neurologic diseases. Hosp Pract 59–71
8. Dickinson AG (1976) Scrapie in sheep and goats. In: Kimberlin RH (ed) Slow virus diseases in animals and man. North-Holland, Amsterdam, pp 210–243
9. Eklund CM, Kennedy RC, Hadlow WJ (1967) Pathogenesis of scrapie virus infection in the mouse. J Infect Dis 117: 15–22
10. Everall IP, Luthert PJ, Lantos PL (1991) Neuronal loss in the frontal cortex in HIV infection. Lancet 337: 1119–1121
11. Ferris CF, Axelson JF, Martin AM, Roberge LF (1989) Vasopressin immunoreactivity in the anterior hypothalamus is altered during the establishment of dominant/subordinate relationships between hamsters. Neuroscience 29: 675–683
12. Fliers E, Swaab DF, Pool CW, Verwer WH (1985) The vasopressin and oxytocin neurons in the human supraoptic and paraventricular nucleus; changes with aging and in senile dementia. Brain Res 342: 45–53
13. Goudsmit E, Fliers E, Swaab DF (1989) Changes in vasopressin neurons and fibers in aging and Alzheimer's disease: reversibility in the rat. In: Iqbal K, Wisniewski HM, Winblad B (eds) Alzheimer's disease and related disorders. Alan R. Liss, New York, pp 1193–1208
14. Goudsmit E, Neijmeijer-Leloux A, Swaab DF (1992) The human hypothalamo-neurohypophyseal system in relation to development, aging and Alzheimer's disease. Prog Brain Res 93: 237–248
15. Hatton GI (1990) Emerging concepts of structure-function dynamics in adult brain: the hypothalamo-neurohypophysial system. Prog Neurobiol 34: 437–504
16. Herman IP, Cullinan WE, Morano MI, Watson SJ (1992) Involvement of the ventral hippocampus in regulation of the hypothalamo-pituitary-adrenocortical axis. Soc Neurosci Abstr 18: 1541
17. Kascsak RJ, Rubenstein R, Carp RI (1991) Evidence for biological and structural diversity among scrapie strains. Curr Top Microbiol Immunol 172: 139–152
18. Kim YS, Carp RI, Callahan SM, Natelli M, Wisniewski HM (1988) Adrenal involvement in scrapie-induced obesity. Proc Soc Exp Biol Med 189: 21–27

19. Kim YS, Carp RI, Callahan SM, Natelli M, Wisniewski HM (1990) Vacuolization, incubation period and survival time analysis in three mouse genotypes injected stereotactically in three brain regions with the 22L scrapie strain. J Neuropathol Exp Neurol 49: 106–113
20. Kimberlin RH (1989) Introduction to scrapie and perspectives on current scrapie research. In: Iqbal K, Wisniewski HM, Winblad B (eds) Alzheimer's disease and related disorders. Alan R. Liss, New York, pp 559–566
21. Lippa CF, Smith TW (1992) The indusium griseum in Alzheimer's disease: an immunocytochemical study. J Neurol Sci 111: 39–45
22. Martignoni E, Petraglia F, Costa A, Genazzani AR, Nappi G (1990) Dementia of the Alzheimer type and hypothalamus-pituitary-adrenocortical axis: changes in cerebrospinal fluid corticotropin releasing factor and plasma cortisol levels. Acta Neurol Scand 81: 452–456
23. Nagashima K, Zabriskie JB, Lyons MJ (1992) Virus-induced obesity in mice: association with a hypothalamic lesion. J Neuropathol Exp Neurol 51: 101–109
24. Oesch B, Westaway D, Wälchli M, McKinley MP, Kent SBH, Aebersold R, Barry RA, Tempst P, Teplow DB, Hood LE, Prusiner SB, Weissmann C (1985) A cellular gene encodes scrapie PrP 27–30 protein. Cell 40: 735–746
25. Palkovits M, Leranth C, Gorcs T, Scott Young W III (1987) Corticotropin-releasing factor in the olivocerebellar trace of rats: demonstration by light- and electron-microscopic immunohistochemistry and in situ hybridization histochemistry. Proc Natl Acad Sci USA 84: 3911–3915
26. Parry HR (1983). In: Oppenheimer DR (ed) Scrapie disease in sheep. Historical, clinical, epidemiological, pathological and practical aspects of the natural disease. Academic Press, London, pp 2–7
27. Peter RE (1986) Vertebrate neurohormonal systems. In: Pang PKT, Schreibman MP (eds) Vertebrate endocrinology: fundamentals and biomedical implications, vol 1. Academic press/ Harcourt Brace Jovanovich, New York, pp 57–104
28. Scott JR, Fraser H (1984) Degenerative hippocampal pathology in mice infected with scrapie. Acta Neuropathol (Berl) 65: 62–68
29. Sidman RI, Angevine JB Jr, Pierce ET (1971) Atlas of the Mouse Brain and Spinal Cord. Harvard University press, Cambridge
30. Swaab DF, Fliers E, Partiman TS (1985) The suprachiasmitic nucleus of the human brain in relation to sex, age and senile dementia. Brain Res 342: 37–44
31. Terry RD (1985) Alzheimer's disease. In: Davis RL, Roberstson DM (eds) Textbook of Neuropathology. Williams and Wilkins, Baltimore, pp 824–841
32. Uno H, Sakai A, Shelton S, Eisele S (1992) Hippocampal regulation of the pituitary-adrenal axis in monkeys. Soc Neurosci Abstr 18: 1541
33. Whitehouse PJ, Vale WW, Zweig RM, Singer HS, Mayeux R, Price DL, De Souza EB (1987) Reductions in corticotropin-releasing factor (CRF)-like immunoreactivity in cerebral cortex in Alzheimer's disease, Parkinson's disease, and progressive supranuclear palsy. Neurology 37: 905–909
34. Whitnall MH (1993) Regulation of the hypothalamic corticotropin-releasing hormone neurosecretory system. Prog Neurobiol 40: 573–629
35. Ye X, Carp RI, Kascsak RJ (1994) Histopathological changes in the islets of Langerhans in scrapie 139H-affected hamsters. J Comp Pathol 110: 153–167
36. Ye X, Carp RI, Yu Y, Kozielski R, Kozlowski P (1994) Hyperplasia and hypertrophy of B cells in the islets of Langerhans in hamsters infected with the 139H strain of scrapie. J Comp Pathol 110: 169–183